Effect of Multiple Adduct Fullerenes on Microstructure and Phase Behavior of P3HT:Fullerene Blend Films for Organic Solar Cells

Anne A. Y. Guilbert,[†,∥] Luke X. Reynolds,[‡,∥] Annalisa Bruno,[‡] Andrew MacLachlan,[‡] Simon P. King,[‡] Mark A. Faist,[†] Ellis Pires,[§] J. Emyr Macdonald,[§] Natalie Stingelin,[⊥] Saif A. Haque,[‡,*] and Jenny Nelson[†,*]

[†]Centre for Plastic Electronics and Department of Physics, Blackett Laboratory, Imperial College London, London SW7 2AZ, United Kingdom, [‡]Centre for Plastic Electronics and Department of Chemistry, Imperial College London, London SW7 2AZ, United Kingdom, [§]School of Physics and Astronomy, Cardiff University, Queens buildings, The Parade, Cardiff CF24 3AA, United Kingdom, and [⊥]Centre for Plastic Electronics and Department of Materials, Royal School of Mines, Imperial College London, London SW7 2AZ, United Kingdom. [∥]These authors contributed equally to this work.

ABSTRACT The bis and tris adducts of [6,6]phenyl-C_{61}-butyric acid methyl ester (PCBM) offer lower reduction potentials than PCBM and are therefore expected to offer larger open-circuit voltages and more efficient energy conversion when blended with conjugated polymers in photovoltaic devices in place of PCBM. However, poor photovoltaic device performances are commonly observed when PCBM is replaced with higher-adduct fullerenes. In this work, we use transmission electron microscopy (TEM), steady-state and ultrafast time-resolved photoluminescence spectroscopy (PL), and differential scanning calorimetry (DSC) to probe the microstructural properties of blend films of poly(3-hexylthiophene-2,5-diyl) (P3HT) with the bis and tris adducts of PCBM. TEM and PL indicate that, in as-spun blend films, fullerenes become less soluble in P3HT as the number of adducts increases. PL indicates that upon annealing crystallization leads to phase separation in P3HT:PCBM samples only. DSC studies indicate that the interactions between P3HT and the fullerene become weaker with higher-adduct fullerenes and that all systems exhibit eutectic phase behavior with a eutectic composition being shifted to higher molar fullerene content for higher-adduct fullerenes. We propose two different mechanisms of microstructure development for PCBM and higher-adduct fullerenes. P3HT:PCBM blends, phase segregation is the result of crystallization of either one or both components and is facilitated by thermal treatments. In contrast, for blends containing higher adducts, the phase separation is due to a partial demixing of the amorphous phases. We rationalize the lower photocurrent generation by the higher-adduct fullerene blends in terms of film microstructure.

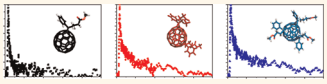

KEYWORDS: organic solar cells · fullerenes · microstructure · phase behavior · TEM · PL · DSC

Organic photovoltaic (OPV) devices have attracted significant attention over the past decade due to their potential for low-cost, scalable fabrication on flexible substrates. The predominant structure for these OPV devices consists of a "bulk heterojunction" formed by a blend of an electron donor and an electron acceptor.[1−3] The best studied example is the blend of poly(3-hexylthiophene-2,5-diyl) (P3HT) as the donor and [6,6]phenyl-C_{61}-butyric acid methyl ester (PCBM) as the acceptor for which device efficiencies around 4−5% are commonly reported.[4−6] Following photogeneration, the exciton diffuses toward a heterojunction where it is separated, leading to the formation of a geminate charge pair. If the geminate charge pair can overcome the mutual Coulombic attraction, the resulting separate polarons can travel toward different electrodes so becoming available for injection in an external circuit. However, numerous undesirable processes such as exciton, geminate pair, and nongeminate charge recombination may also occur, and these energy losses can be either radiative or nonradiative. In addition, part of the exciton energy is lost during the formation of the geminate pair. In attempts to increase the amount of light harvested and to reduce the energy lost at this stage, new polymer donors and acceptor materials with varying electronic energy levels have been synthesized. New low-band-gap polymer donors have resulted in efficiencies over 8%,[7] partly as a result of a broader absorption profile leading to an increase in photocurrent and partly due to improved energy level alignment.

In contrast to the wide variety of p-type polymers under development, fullerenes remain the acceptors of choice in the best performing OPV devices. Recently, a number of new fullerene derivatives have been synthesized in order to enhance device performances. The main strategy has been to raise the fullerene lowest unoccupied molecular orbital (LUMO) level through side group attachment, leading to a decreased

* Address correspondence to jenny.nelson@imperial.ac.uk, s.a.haque@imperial.ac.uk.

Received for review December 20, 2011 and accepted April 25, 2012.

Published online April 25, 2012
10.1021/nn204996w

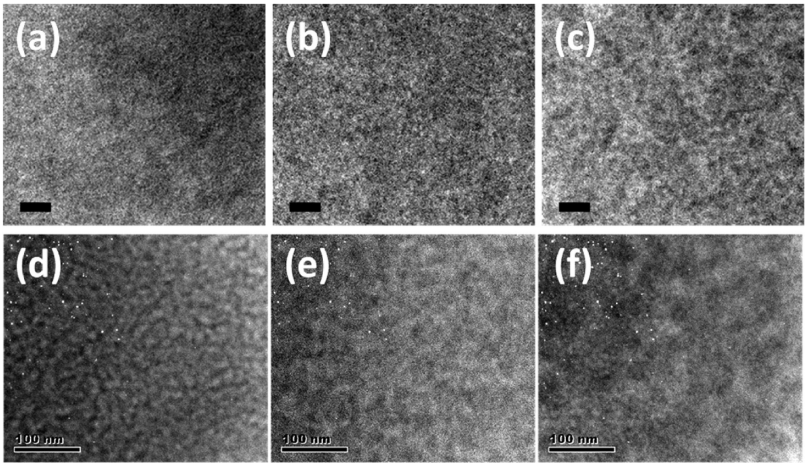

Figure 1. TEM micrographs of as-spun (a−c) and annealed (d−f) 50 wt % (∼85 mol %) P3HT blend films of P3HT:PCBM (a,d), P3HT:bis-PCBM (b,e), and P3HT:tris-PCBM (c,f). All scale bars represent 100 nm.

electrochemical loss when charges are transferred from polymer to fullerene and a concomitant increase in V_{oc}.[8] In the case of the bis and tris adducts of PCBM (in the following, they will be referred to as bis- and tris-PCBM), the LUMO level is raised relative to PCBM by about 110 and 220 meV, respectively.[9−12] Upon replacing PCBM with bis-PCBM in blends with P3HT, a significant increase in V_{oc} has been indeed observed, albeit with a slight decrease in short-circuit current (J_{sc}).[10−12] When bis-PCBM is replaced with tris-PCBM, a slight increase in V_{oc} is again observed but J_{sc} reduces drastically.[10−12] Since no significant decrease in charge generation has been found with higher-adduct fullerenes,[12] the decrease in J_{sc} for blends containing higher-adduct fullerenes and the relatively small effect of LUMO level rise on V_{oc} in the case of tris-PCBM have been attributed to the decrease in electron mobility of the higher-adduct fullerenes in comparison to PCBM.[10−12] In addition, it has been argued that the three fullerenes feature different blend microstructures; thermal annealing leads to the appearance of micrometer-sized fullerene aggregates in the case of PCBM only, while blend films containing the higher-adduct fullerenes remain essentially featureless.[12] Even more pronounced differences in microstructure have been observed when the fullerene derivatives were used in combination with polymers such as poly(2-methoxy-5-(3′-7′-dimethyloctyloxy)-1,4-phenylenevinylene) (MDMO-PPV) and poly[(9,9-dioctylfluorenyl-2,7-diyl)-*co*-5,5-4′,7′-di-2-thienyl-2′,1′,3′-benzothiadiazole] (APFO-3). In particular, bis-PCBM blended with the latter two polymers results in poor solar cell performances in comparison with PCBM-based devices, in contrast to the case of P3HT-based blends. Since MDMO-PPV and APFO-3 are less crystalline than P3HT, the poorer device performances suggest that the effect of bis-PCBM on solar cell performance may be related to the tendency of the polymers to crystallize.[13] Crystallization is known to drive phase separation processes, while the amorphous (or molecularly less ordered) regions of the donor polymers can accommodate a large fraction of solubilized acceptor molecules.[14] These observations are consistent with other studies which demonstrate that bulk heterojunction solar cells exhibit a strong dependence of the power conversion efficiency upon composition and processing conditions (such as thermal treatment), suggesting that the active layer microstructure indeed plays a critical role in the performance of devices.[15−18]

In this paper, we focus on the P3HT:fullerene system in order to understand the effect of the fullerene chemical structure on the blend microstructure development. We consider the miscibility of the fullerenes with P3HT in the solid state and the extent of phase separation. We relate the phase behavior of the P3HT:fullerene blends with the device performances reported previously.[10,11] For this purpose, we use transmission electron microscopy (TEM) and steady-state and ultrafast time-resolved photoluminescence (PL) spectroscopy to characterize the microstructure of P3HT:PCBM, P3HT:bis-PCBM, and P3HT:tris-PCBM blends. This is complemented by differential scanning calorimetry (DSC) which is used to investigate the phase behavior of blends of P3HT with PCBM and its higher adducts, so establishing temperature−composition phase diagrams for the individual binary systems.

RESULTS AND DISCUSSION

Characterization of the Blend Morphology. TEM micrographs of as-spun and annealed P3HT:fullerene films comprising 50 wt % P3HT (∼85 mol % P3HT)[19] are displayed in Figure 1. A clear trend is observed for the as-spun films, namely, that the blends containing higher-adduct fullerenes feature a rougher phase separation compared to P3HT:PCBM binaries. Thermal treatment promotes phase separation for P3HT:PCBM,

while no significant change is observed for blends containing higher-adduct fullerenes. However, no quantitative information on either the domain composition or on the domain size can be deduced from the TEM data.

Steady-state photoluminescence spectroscopy has previously been used to infer the degree of phase separation in blends. In a similar manner, we have performed steady-state PL measurements of blend films of different polymer:fullerene ratios (see Supporting Information). No variation in the shape of the polymer emission spectrum is observed upon adding fullerenes, implying that the emission between 640 and 696 nm is due solely to the polymer and not to any other species such as a charge transfer state. Therefore, any difference in quenching ability could be attributed to one or more of three effects: a difference in polaron generation yield, a difference in nonradiative decay pathways, or a difference in microstructure. Since steady-state PL provides us with the time-integrated PL signal, it cannot distinguish between the decay mechanisms responsible for P3HT emission quenching. Therefore, we have also performed ultrafast time-resolved PL spectroscopy measurements using the fluorescence up-conversion technique. Ultrafast PL spectroscopy has the advantage of allowing the direct observation of the emissive decay dynamic of the initial excited-state species in these blend films.

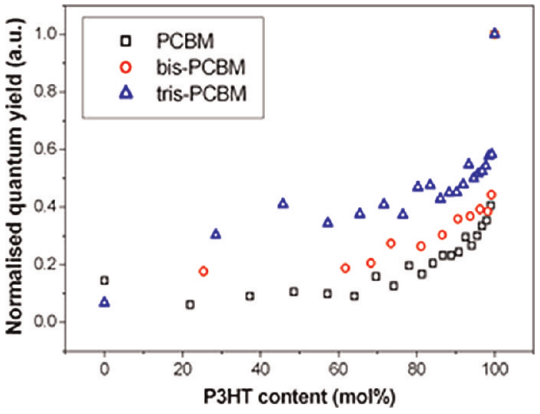

Figure 2. Normalized quantum yield of as-spun P3HT:fullerene films of different compositions. The excitation wavelength was 510 nm, and the fluorescence yield was calculated between 640 and 696 nm. Raw absorption and PL spectra are available in the Supporting Information.

In Figure 2, the normalized quantum yield (the number of emitted photons—calculated by integrating the steady-state PL spectra between 640 and 696 nm—divided by the absorbed photons at 510 nm) is plotted for blends of P3HT and the three fullerenes as a function of the P3HT content. The quenching of the polymer emission in as-spun blends comprising all three fullerenes is seen to become more efficient upon increasing the acceptor content. However, for blends of the same acceptor content, it is evident from our data that PCBM consistently quenches the polymer emission more than bis-PCBM, which in turn quenches much more than tris-PCBM. The same trend is observed in the initial peak intensity of the ultrafast PL (see Supporting Information). In contrast, for the annealed films, the intensity ratio is similar for all fullerenes (see Supporting Information).

The ultrafast time-resolved emission decay traces are plotted in Figure 3. Comparing the time decay curves, it can be observed that PCBM quenches the polymer emission more efficiently than bis-PCBM, which in turn quenches the polymer emission more efficiently than tris-PCBM. The time-resolved photoluminescence decays are not monoexponential but can be well modeled with a sum of two exponentials suggesting phenomena on different time scales.[20−22] The fast (<3 ps) and slow (>3 ps) time decays are plotted as a function of the blend composition in Figure 4. The fast-phase dynamics remain constant over all blend compositions, whereas the slow-phase time decay decreases upon increasing the relative content of quencher. In addition, it is observed that even at low fullerene contents (99 mol % P3HT) the PL is quenched more slowly for blends comprising higher-adduct fullerenes (as has been shown previously for PCBM and bis-PCBM),[23] and this difference in quenching efficiency increases when increasing the fullerene content. Upon annealing, decay times observed for P3HT:PCBM blends are lengthened, while the decay times observed for P3HT blended with higher adducts seem not to be significantly affected by the annealing

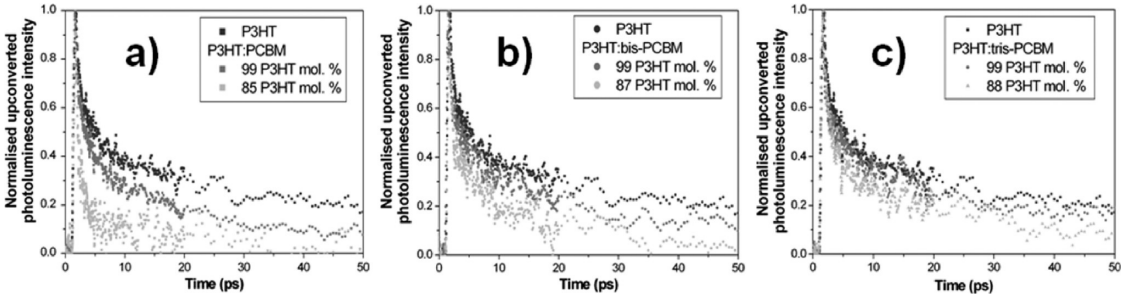

Figure 3. Ultrafast time-resolved emission decay traces of as-spun blends of (a) P3HT:PCBM, (b) P3HT:bis-PCBM, and (c) P3HT:tris-PCBM. The excitation wavelength was 400 nm, and the P3HT emission was detected at 650 nm.

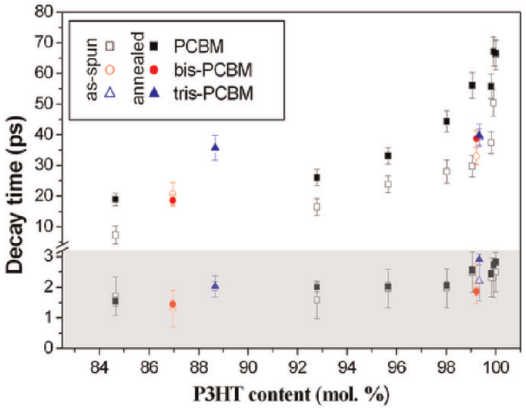

Figure 4. Time components of the biexponential decay fits to the ultrafast fluorescence up-conversion decays for as-spun (open shapes) and annealed (solid shapes) films showing the fast-phase decay rate (<3 ps) and the slow-phase decay rate (>3 ps).

procedure. As a result, after annealing, decay times for films containing high loadings of PCBM and bis-PCBM are similar while those for tris-PCBM remain longer.

The observed difference in quenching ability of the fullerenes could, in principle, be attributed to the differing electron affinities of the fullerenes and hence different driving forces for electron transfer. However, even for P3HT:tris-PCBM, the LUMO energy difference is ~0.8 eV, which far exceeds the 0.3−0.5 eV thought to be needed for efficient charge separation;[24] indeed, similar polaron generation yields have been observed for blend films of P3HT with all three fullerenes.[12] We note that some differences in quenching ability could arise from variations in charge transfer rate due to variations in the donor−acceptor interface distances. However, in studies of similar polymer:fullerene systems, differences in quenching have been mainly attributed to microstructure,[25] a conclusion further supported by the transient absorption data on P3HT:PCBM and bis- and tris-PCBM published by Faist *et al.*[12] Further insight is provided by the independence of the fast phase of the ultrafast PL decay data on the fullerene adduct. This fast phase has previously been related to the changes in conformation of P3HT polymer chains.[20,26] The fact that the fast-phase decay remains constant over all blend compositions and with all three fullerene acceptors suggests that the nonradiative decay pathways are similar for all three fullerene acceptors and so are unlikely to be responsible for any difference in quenching ability between the three fullerenes. Therefore, the difference in quenching ability is more likely to be due to a difference in microstructure.

Since steady-state PL provides us with the time-integrated PL signal, it is very sensitive to the initial (<150 fs) PL intensity and less to the decay, which explains why the trends, observed by steady-state PL and the amplitude of the initial peak intensity of the ultrafast PL, are similar. This pre-150 fs time scale quenching is more likely to be due to the fraction of excitons that are formed within the quenching radius of fullerenes.[27] Thus, the less quenched polymer emission for as-spun blends comprising higher adducts suggests that the higher adducts are less well-dispersed within P3HT. Since there is no evidence of fullerene intercalation (or cocrystallization) with P3HT as deduced from grazing-incidence X-ray diffraction (GIXRD) (see Figures 4 and 5 in Supporting Information) and since the crystalline domains of P3HT:PCBM derivative blends are on average of a similar size as deduced from GIXRD (see Table 2 in Supporting Information), it is likely to be the solubility of the fullerene derivatives in the amorphous phase of P3HT that differs. The reduction of these ultrafast losses by thermal treatment leading to a similar PL intensity for all three fullerenes suggests that after annealing all three fullerenes are dispersed to a comparable extent within P3HT.

The slow phase observed in ultrafast spectroscopy may be attributed to exciton hopping processes between segments of the same polymer chain or to segments of an adjacent chain and so reflects the diffusive movement of the exciton before it reaches a polymer:fullerene heterojunction.[28,29] In as-spun films, the lengthening of the slow-phase decay by replacing PCBM with higher-adduct fullerenes points toward a longer average distance from the point of exciton generation to a heterojunction in higher-adduct blends than in P3HT:PCBM. After annealing, excitons in blends containing PCBM and bis-PCBM travel on average the same distance before being dissociated, and this distance remains shorter than the average distance that an exciton has to travel in P3HT:tris-PCBM blends to reach a heterojunction.

Thermal annealing is known to promote demixing in P3HT:PCBM system through crystallization-driven phase segregation.[30] This is consistent with our photophysical data. However, in as-spun films, rougher phase separation of blends containing higher-adduct fullerenes has been observed by TEM, while P3HT crystallinity, as probed by GIXRD (see Figure 5 and Table 2 in Supporting Information), is similar for blends containing all three fullerene derivatives. Therefore, demixing cannot solely be driven by crystallization. From our steady-state and ultrafast PL data, we propose a second demixing mechanism, namely, demixing within the amorphous phase of as-spun blends containing higher-adduct fullerenes. This demixing is due to less solubility of higher-adduct fullerenes within the amorphous phase of P3HT. In other words, it is likely that crystalline P3HT, a fullerene amorphous phase, a P3HT amorphous phase, and a "solid solution" of molecularly relatively unordered fullerenes and P3HT coexist in the blends containing higher-adduct fullerenes. Furthermore, thermal treatments do not

seem to affect the microstructure of P3HT:tris-PCBM blends and only slightly affect P3HT:bis-PCBM blends. This is consistent with a phase segregation in blends containing higher-adduct fullerenes occurring in the amorphous phase and being almost independent of crystallization processes. Because steady-state PL but not ultrafast dynamics is slightly affected by thermal annealing in the case of bis-PCBM, it cannot be excluded that during annealing some bis-PCBM diffuses through P3HT amorphous phase to form some small crystallites. This diffusion process, which is expected to be of small extent, should lead to slightly less bis-PCBM dissolved in the P3HT amorphous phase but should not modify the distance an exciton has, on average, to travel from the photoexcitation location to a heterojunction. Schematics depicting the microstructures of the various blends, as-spun and annealed, in agreement with our photophysical and TEM data are presented in Scheme 1. The observed difference in microstructure reflected by our photophysical study can be explained in terms of weaker interactions between the polymer and higher-adduct fullerenes compared to those that exist between the polymer and lower-adduct fullerenes. In the following section, we will use thermal analysis to study the polymer:fullerene interactions.

Characterization of the Phase Behavior. The photophysical study described above provides a valuable insight into the difference between P3HT:PCBM and bis- and tris-PCBM blend films in term of microstructure and suggests that the fullerene−P3HT molecular interaction is altered by modifying the chemical structure of the fullerene. Further information can be obtained from thermal analysis, especially DSC. Müller *et al.*[31] found using DSC that the P3HT:PCBM system exhibits a eutectic phase behavior with a eutectic composition at 91 mol % P3HT and a eutectic temperature around 200 °C. In the present work, blends of P3HT with higher-adduct fullerenes have been analyzed using identical procedures; the resulting DSC thermographs of P3HT:bis-PCBM and P3HT:tris-PCBM blends are plotted in Figure 5. In contrast to PCBM, no melting endotherm corresponding to either bis-PCBM or tris-PCBM is observed (see Supporting Information), illustrating the low tendency to crystallize of these two PCBM derivatives.[12,32] However, for both systems, the addition of fullerenes results in a noticeable depression of the melting temperature of P3HT as previously observed adding PCBM to P3HT.[31] The effect is stronger for blends of P3HT and bis-PCBM than for P3HT:tris-PCBM and stronger still for P3HT:PCBM, indicating stronger interactions between the two components in P3HT:PCBM blends than in P3HT:bis-PCBM and P3HT:tris-PCBM binaries.

From our thermal analysis, we further conclude that, similar to the P3HT:PCBM system, bis- and tris-PCBM when blended with P3HT exhibit a eutectic phase behavior. This is evident from the endotherms observed at approximately 210 and 220 °C for blends based on bis- and tris-PCBM, respectively (leading at higher polymer concentrations to an endothermic "shoulder" at the low-temperature regime of the P3HT melting endotherm) (Figure 5). In order to better resolve the eutectic temperature, additional DSC runs have been performed using a heating rate of 2 °C/min (see Supporting Information). On the basis of this data set, the eutectic composition and temperature can be assigned to be 80 mol % P3HT and 225 °C for P3HT:bis-PCBM blends and lower than 65 mol % P3HT and

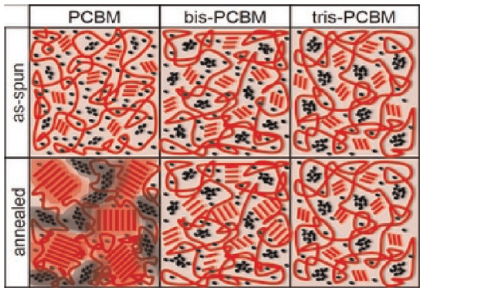

Scheme 1. Schematics depicting the proposed microstructure of as-spun and annealed films of P3HT:PCBM, P3HT:bis-PCBM, and P3HT:tris-PCBM.

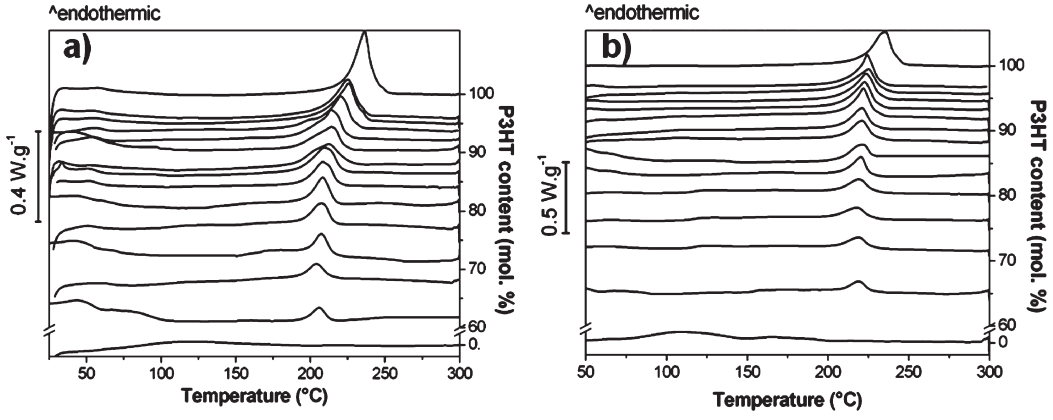

Figure 5. DSC scans of (a) P3HT:bis-PCBM and (b) P3HT:tris-PCBM films of different compositions at a heating rate of 10 °C/min.

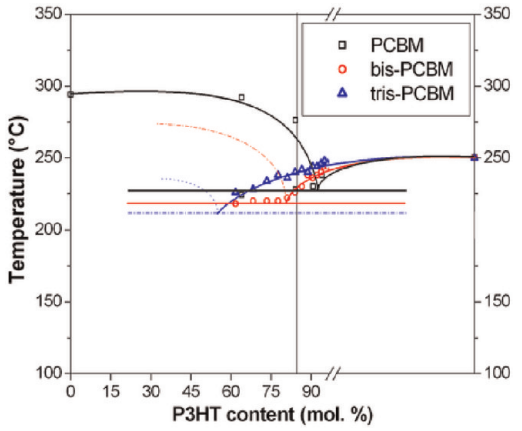

Figure 6. P3HT:PCBM, P3HT:bis- and tris-PCBM non-equilibrium phase diagrams. The points are the melting temperatures extracted from the DSC scans. The dashed lines are extrapolated. The vertical line corresponds to a composition of 50 wt % P3HT.

220 °C for P3HT:tris-PCBM. For comparison, the eutectic composition for P3HT:PCBM is 91 mol % at a temperature of 200 °C (Figure 6). The fact that the eutectic composition is shifted to higher fullerene content and the eutectic temperature is lowered when increasing the number of side chains attached to the fullerene cage may result from both weaker interactions between fullerene and P3HT[12,32] as well as lower fullerene melting temperature.

It should be noted that compositions of slightly lower polymer content than the eutectic composition are usually found to be attractive for high solar cell performance because at these particular compositions the finest phase separation of the crystalline parts of the two components can be expected, and this is combined with the presence of fullerene "primary crystals". The excess fullerene is expected to enhance the electron mobility within the percolation pathway, while hole percolation is still facilitated by the polymer component of the mixed phase.[26] While a P3HT content of 85 mol % (50 wt % P3HT) is in the hypo-eutectic regime for P3HT:PCBM blends, P3HT contents of 85 mol % are in the hyper-eutectic regime for blends comprising higher-adduct fullerenes. Therefore, the primary crystals of fullerene that appear to be critical for efficient electron transport are less likely to form and electron collection may therefore be limited. Indeed, device measurements show that annealed blends containing bis-PCBM require a higher fullerene content to maximize the photocurrent (see Supporting Information). This may explain, at least partially, the small decrease in J_{sc} observed when replacing PCBM with bis-PCBM in blends of 50 wt % polymer and the larger decrease in J_{sc} when replacing bis-PCBM with tris-PCBM[12] and helps to explain why blends with higher adducts require a larger fullerene content to enhance device performances.[10,11]

CONCLUSIONS

We have used a complementary set of techniques to elucidate the microstructure development and the phase behavior of blends of P3HT and fullerene derivatives. TEM reveals a rougher phase separation for the higher-adduct fullerenes for as-spun blends. This rougher phase separation is found to result from the lower solubility of higher-adduct fullerenes in the amorphous phase of P3HT. This can be deduced from the fact that higher-adduct fullerenes lead to less efficient PL quenching than observed for P3HT:PCBM, while no evidence of cocrystallization was found in GIXRD, and the crystalline P3HT domain sizes are similar for all three systems. Thermal treatment promotes demixing of P3HT:PCBM as evidenced through the TEM micrographs, the decrease of PL quenching, and the lengthening of the decay times. In contrast, only small changes are observed for blends containing higher-adduct fullerenes during the annealing procedure (the PL quenching of bis-PCBM decreases slightly, while the PL quenching of tris-PCBM remains essentially identical to the one of as-spun films). Annealing procedures do not lead to further phase separation in the case of higher-adduct fullerene-based blends. This has been explained by the comparatively low solubility of bis- and tris-PCBM in P3HT, as well as their low tendency to crystallize. Therefore, we propose that the origins of phase separation are different in the three systems. In P3HT:PCBM blends, the two components phase segregate due to crystallization of one if not both components as facilitated by thermal treatments. In contrast, for blends containing higher adducts, the phase separation originates from the low solubility of the fullerenes in the amorphous phase of P3HT, leading to at least partial demixing of the amorphous phases. The low solubility of higher-adduct fullerenes in the amorphous polymer fractions has been related to weaker interactions between fullerenes and polymer (evidenced through the lower P3HT melting point depression). The weaker interactions of P3HT with the higher-adduct fullerenes are thought to at least partly explain the shift of the eutectic composition toward higher fullerene content as well as the lower eutectic temperature found for these binaries compared to P3HT:PCBM. This variation of eutectic composition (50 wt % P3HT is in the hyper-eutectic part of the phase diagram) leads to a lack of fullerene crystals that are thought to be essential to enhance the electron mobility within the percolation pathway. This limits the electron collection, which can explain the observed decrease in J_{sc} when replacing PCBM by either bis-PCBM or tris-PCBM. To conclude, we have found two mechanisms of microstructure development within blends of P3HT with PCBM, bis-PCBM, and tris-PCBM. The first originates from crystallization through thermal annealing and leads to high solar cell

performances, while the second originates from the low solubility of fullerenes within the amorphous phase of the polymer and leads to poorer solar cell performances even after annealing procedures.

EXPERIMENTAL SECTION

Materials and Solutions. PCBM, bis-, and tris-PCBM were supplied by Solenne BV with molecular weights of 910.88, 1101.10, and 1291.32 g/mol, respectively. P3HT was obtained from Merck Chemicals (RR = 94.7%, M_n = 19.5 kg/mol, M_w = 34.1 kg/mol, PD = 1.74), and all chemicals were used as received. Thin films for spectroscopy were fabricated by spin-coating of material mixtures (10 mg/mL) from chlorobenzene onto quartz substrates.

Absorption and Photoluminescence. Steady-state UV−vis absorption and time-integrated PL spectroscopic data were measured using a Perkin-Elmer Lamda 25 spectrophotometer and a Horiba Jobin Yvon Fluorolog-2 PL spectrometer, respectively. Ultrafast time-resolved photoluminescence decays were measured using the femtosecond up-conversion technique. The samples were held in a nitrogen atmosphere and continuously translated through the excitation beam to eliminate photobleaching effects and local degradation of the films. Excitation was below the onset of intensity-dependent kinetics and was performed with the frequency-doubled output of a mode-locked Ti:sapphire laser supplying 70 fs pulses at 800 nm with a repetition rate of 80 MHz. The emission at 650 nm was up-converted in a beta-barium-borate crystal using the fundamental laser beam at 800 nm as the gate. Sum-frequency photons were dispersed in a monochromator and detected using a photomultiplier tube. The temporal resolution of the system was ∼150 fs.

Transmission Electron Microscopy. For TEM images, the P3HT:fullerene films were floated onto the surface of deionized water and caught on 300 mesh copper grids. TEM images were obtained using a JEOL 2000FX electron micrograph operated at 200 kV.

Differential Scanning Calorimetry. Thin films were drop-cast from the homogeneous solutions onto glass slides, followed by evaporation of the solvent at room temperature. Afterward, the thin films were scratched, and the "powder" was placed in aluminum pans to be analyzed. The sample weight was about 5 mg. DSC was conducted under nitrogen at three different heating rates: 2, 10, and 20 °C/min and a cooling rate of −10 °C/min with a Metler Toledo DSC822 instrument.

Grazing-Incidence X-ray Diffraction. Samples were prepared by spin-coating the respective solutions onto 1 mm thick silicon substrates (IDB Technologies), resulting in films between 95 and 130 nm thick. The GIXRD technique has been reviewed previously.[15,33] GIXRD measurements were performed at the I07 beamline (Diamond Light Source, UK). A chamber containing a hot plate, on which the samples were glued with conductive silver paint, and a system of motorized shields and slits to reduce the background noise, was mounted on a 2 + 3 circle diffractometer with a hexapod sample stage. The chamber was filled with helium before the experiments started to avoid air scattering. A monochromatic radiation of 10 keV energy and resolution of $<1 \times 10 - 4$ keV were used. Diffraction patterns were detected with a PILATUS 100K (Dectris) Si photodiode array detector. Single images were collected every 7.45 ± 0.25 s, as a compromise between high signal-to-noise ratio and high sampling rate. After aligning the sample and detecting the critical angle, a standardized set of scans was performed for all of the samples.

Conflict of Interest: The authors declare no competing financial interest.

Acknowledgment. This work was supported by EPRSC (EP/G031088, EP/J500021/1, and EP/H040218/1) and the SUPERGEN Excitonic Solar Cell Consortium. The authors would like to thank P. Smith for fruitful discussions, as well as T. Agostinelli, E. Buchaca Domingo, J. Nekuda Malik, and L. Yu for their help. J.N. acknowledges the award of an Industry Fellowship from the Royal Society. S.A.H. acknowledges the award of a University Research Fellowship from the Royal Society.

Supporting Information Available: Additional figures contain UV−vis absorption spectra, steady-state PL spectra, ultrafast PL initial fluorescence intensity, GIXRD data and analysis of P3HT:PCBM, P3HT:bis-PCBM, and P3HT:tris-PCBM blends, DSC scans of blends of P3HT:bis-PCBM and P3HT:tris-PCBM at different compositions, and device characteristics for P3HT:bis-PCBM blends at different compositions. This material is available free of charge *via* the Internet at http://pubs.acs.org.

REFERENCES AND NOTES

1. Sariciftci, N. S.; Smilovitz, L.; Heeger, A. J.; Wudl, F. Photoinduced Electron Transfer from a Conducting Polymer to Buckminsterfullerene. *Science* **1992**, *258*, 1474.
2. Halls, J. J. M.; Walsh, C. A.; Greenham, N. C.; Marseglia, E. A.; Friend, R. H.; Moratti, S. C.; Holmes, A. B. Efficient Photodiodes from Interpenetrating Polymer Networks. *Nature* **1995**, *376*, 498.
3. Yu, G.; Heeger, A. J. Charge Separation and Photovoltaic Conversion in Polymer Composites with Internal Donor/Acceptor Heterojunctions. *J. Appl. Phys.* **1995**, *78*, 4510–4515.
4. Li, G.; Shrotriya, V.; Huang, J.; Yao, Y.; Moriarty, T.; Emery, K.; Yang, Y. High-Efficiency Solution Processable Polymer Photovoltaic Cells by Self-Organisation of Polymer Blends. *Nat. Mater.* **2005**, *4*, 864.
5. Reyes-Reyes, M.; Kim, K.; Carroll, D. L. High-Efficiency Photovoltaic Devices Based on Annealed Poly(3-hexylthiophene) and 1-(3-Methoxycarbonyl)-propyl-1-phenyl-(6,6)C_{61} Blends. *Appl. Phys. Lett.* **2005**, *87*, 083506.
6. Ma, W.; Yang, C.; Gong, X.; Lee, K.; Heeger, A. J. Thermal Stable, Efficient Polymer Solar Cells with Nanoscale Control of the Interpentrating Network Morphology. *Adv. Funct. Mater.* **2005**, *15*, 1617–1622.
7. Liang, Y.; Xu, Z.; Xia, J.; Tsai, S.-T.; Wu, Y.; Li, G. For the Bright Future: Bulk Heterojunction Polymer Solar Cells with Power Conversion Efficiency of 7.4%. *Adv. Energy Mater.* **2010**, *22*, E135.
8. Koster, L. J. A.; Mihailetchi, V. D.; Blom, P. W. M. Ultimate Efficiency of Polymer/Fullerene Bulk Heterojunction Solar Cells. *Appl. Phys. Lett.* **2006**, *88*, 093511.
9. Diederich, F.; Kessinger, R. Templated Regioselective and Stereoselective Synthesis in Fullerene Chemistry. *Acc. Chem. Res.* **1999**, *32*, 537–545.
10. Lenes, M.; Wetzelaer, G.-J. A. H.; Kooistra, F. B.; Veenstra, S. C.; Hummelen, J. C.; Blom, P. W. M. Fullerene Bisadducts for Enhanced Open-Circuit Voltages and Efficiencies in Polymer Solar Cells. *Adv. Mater.* **2008**, *20*, 2116–2119.
11. Lenes, M.; Shelton, S. W.; Sieval, A. B.; Kronholm, D. F.; Hummelen, J. C.; Blom, P. W. M. Electron Trapping in Higher Adduct Fullerene-Based Solar Cells. *Adv. Funct. Mater.* **2009**, *19*, 3002–3007.
12. Faist, M. A.; Keivanidis, P. E.; Foster, S.; Woebkenberg, P. H.; Anthopoulos, T. D.; Bradley, D. D. C.; Durrant, J. R.; Nelson, J. Effect of Multiple Adduct Fullerenes on Charge Generation and Transport in Photovoltaic Blends with Poly(3-hexylthiophene-2,5-diyl). *J. Polym. Sci., Part B: Polym. Phys.* **2011**, *49*, 45–51.
13. Faist, M. A.; Kirchartz, T.; Gong, W.; Ashraf, R. S.; McCulloch, I.; de Mello, J. C.; Ekins-Daukes, N.; Bradley, D. D. C.; Nelson, J. Competition between the Charge Transfer State and the Singlet States of Donor or Acceptor Limiting the Efficiency

in Polymer:Fullerene Solar Cells. *J. Am. Chem. Soc.* **2012**, *134*, 685–692.
14. Collins, B. A.; Gann, E.; Guignard, L.; He, X.; McNeill, C. R.; Ade, H. Molecular Miscibility of Polymer−Fullerene Blends. *J. Phys. Chem. Lett.* **2010**, *1*, 3160–3166.
15. Kim, Y.; Cook, S.; Tuladhar, S. M.; Choulis, S. A.; Nelson, J.; Durrant, J. R.; Bradley, D. D. C.; Giles, M.; McCulloch, I.; Ha, C. S.; *et al.* A Strong Regioregularity Effect in Self-Organizing Conjugated Polymer Films and High-Efficiency Polythiophene:Fullerene Solar Cells. *Nat. Mater.* **2006**, *5*, 197–203.
16. Rait, S.; Kashyap, S.; Bhatnagar, P. K.; Mathur, P. C.; Sengupta, S. K.; Kumar, J. Improving Power Conversion Efficiency in Polythiophene/Fullerene-Based Bulk Heterojunction Solar Cells. *Sol. Energy Mater. Sol. Cells* **2007**, *91*, 757–763.
17. Clarke, T. M.; Ballantyne, A. M.; Nelson, J.; Bradley, D. D. C.; Durrant, J. R. Free Energy Control of Charge Photogeneration in Polythiophene/Fullerene Solar Cells: The Influence of Thermal Annealing on P3HT/PCBM Blends. *Adv. Funct. Mater.* **2008**, *18*, 4029–4035.
18. Keivanidis, P. E.; Clarke, T. M.; Liliu, S.; Agostinelli, T.; Macdonald, J. E.; Durrant, J. R.; Bradley, D. D. C.; Nelson, J. Dependence of Charge Separation Efficiency on Film Microstructure in Poly(3-hexylthiophene-2,5-diyl):[6,6]-Phenyl-C61 Butyric Acid Methyl Ester Blend Films. *J. Phys. Chem. Lett.* **2010**, *1*, 734–738.
19. Mol % P3HT will be used from here on for clarity and refers to the ratio of the number of moles of 3HT monomers to the total number of moles in the blend.
20. Parkinson, P.; Müller, C.; Stingelin, N.; Johnson, M. B.; Herz, L. M. Role of Ultrafast Torsional Relaxation in the Emission from Polythiophene Aggregates. *J. Phys. Chem. Lett.* **2010**, *1*, 2788–2792.
21. Xie, Y.; Li, Y.; Xiao, L.; Qiao, Q; Dhakal, R.; Zhang, Z.; Gong, Q.; Galipeau, D.; Yan, X. Femtosecond Time-Resolved Fluorescence Study of P3HT/PCBM Blend Films. *J. Phys. Chem. C* **2010**, *114*, 14590–14600.
22. Banerji, N.; Cowan, S.; Vauthey, E.; Heeger, A. J. Ultrafast Relaxation of the Poly(3-hexylthiophene) Emission Spectrum. *J. Phys. Chem. C* **2011**, *115*, 9726–9739.
23. Jarzab, D.; Cordella, F.; Lenes, M.; Kooistra, F. B.; Blom, P. W. M.; Hummelen, J. C.; Loi, M. A. Charge Transfer Dynamics in Polymer-Fullerene Blends for Efficient Solar Cells. *J. Phys. Chem. B* **2009**, *113*, 16513–16517.
24. Halls, J. J. M.; Cornil, J.; Dos Santos, D. A.; Silbey, R.; Hwang, D. H.; Holmes, A. B.; Bredas, J. L.; Friend, R. H. Charge- and Energy-Transfer Processes at Polymer/Polymer Interfaces: A Joint Experimental and Theoretical Study. *Phys. Rev. B* **1999**, *60*, 5721.
25. Bruno, A.; Reynolds, L. X.; Dyer-Smith, C.; Bradley, D. D. C.; Nelson, J.; Haque, S. A. Determining the Exciton Diffusion Length in a Polyfluorene from Ultrafast Fluorescence Measurements of Polymer:Fullerene Blend Films. Submitted for publication.
26. Dykstra, T.; Hennebicq, E.; Beljonne, D.; Gierschner, J.; Claudio, G.; Bittner, E.; Knoester, J.; Scholes, G. D. Conformatial Disorder and Ultrafast Exciton Relaxation in PPV-Family Conjugated Polymers. *J. Phys. Chem. B* **2009**, *113*, 656–667.
27. Trotsky, S.; Hoyer, T.; Tuszynski, W.; Lienau, C.; Parisi, J. Femtosecond Up-Conversion Technique for Probing the Charge Transfer in a P3HT:PCBM Blend *via* Photoluminescence Quenching. *J. Phys. D: Appl. Phys.* **2009**, *42*, 055105.
28. Wells, N.; Boudouris, B.; Hillmyer, M.; Blank, M. Intermolecular Exciton Relaxation and Migration in Poly(3-hexylthiophene). *J. Phys. Chem. C* **2007**, *111*, 15404–15414.
29. Ruseckas, A.; Samuel, I.; Shaw, P. Probing the Nanoscale Phase Separation in Binary Photovoltaic Blends of Poly(3-hexylthiophene) and Maethanofullerene by Energy Transfer. *Dalton Trans.* **2009**, *45*, 10040–10043.
30. Padinger, F.; Rittberger, R. S.; Sariciftci, N. S. Effects of Postproduction Treatment on Plastic Solar Cells. *Adv. Funct. Mater.* **2003**, *13*, 85–88.
31. Müller, C.; Ferenczi, T. A. M.; Campoy-Quiles, M.; Frost, J. M.; Bradley, D. D. C.; Smith, P.; Stingelin-Stutzmann, N.; Nelson, J. Binary Organic Photovoltaic Blends: A Simple Rationale for Optimum Compositions. *Adv. Mater.* **2008**, *20*, 3510–3515.
32. MacKenzie, R. C. I.; Frost, J. M.; Nelson, J. A Numerical Study of Mobility in Thin Films of Fullerene Derivatives. *J. Chem. Phys.* **2010**, *132*, 064904.
33. Birkholz, M. *Thin Film Analysis by X-ray Scattering*; Wiley-VCH Verlag GmbH & Co.: Weinheim, Germany, 2006.